

The detail design of hollow clevis-pin type of load cells.

Surasith Piyasin, Ph.D.

Department of Mechanical Engineering

Khon Kaen University, Khon Kaen , 40002

Tel. 043-244296, Fax. 043-245878, Email:surasith@kku.ac.th

Keywords : Clevis-pin, FEM, Load cells

Abstract.

The object of this paper is to describe the strain/stress distribution from internal surface of a hollow clevis-pin. Finite element method using ANSYS has been used as the core of this investigation. The work has shown how certain geometric proportion for the hollow-bore clevis-pin and also how certain positions for the strain gauges offer some advantages over the proportions and gauge positions.

1. Introduction.

Clevis-pins are widely used in heavy-duty machinery such as cranes, hoists, conveyors, etc. In order to access the load capacity of a clevis-pin, some knowledge of strain/stress field within a hollow-bore is required. For this reason, using finite element method to receive the strain/stress distribution of internal surface of a hollow-bore cylinder will lead to the selection and assessment of critical position and orientations for strain gauge elements.

In existing designs of a U.S. Patent no. 3,695,096, there is only geometric feature is shown. However some technical data supports with enable to criticise to optimum value of strain patterns and also their positions, are not all clear.

2. Clevis-pin load cell subject to general stress/strain distributions.

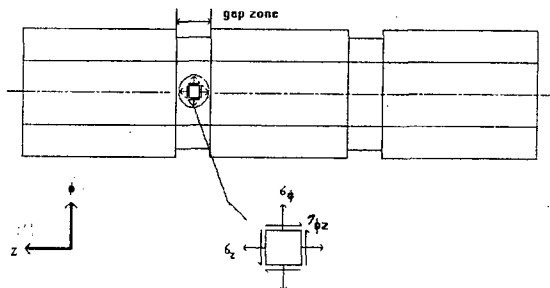


Fig.1: The general arrangement hollow-bore clevis-pin and the supposed arrangement of the strain gauge.

Consider an axisymmetric hollow cylinder with distribution loads on the mid-'depth' flank surfaces. The shear force diagram and moment force diagram are shown as in Fig.2. These forces and moments generate stress distributions over the internal and external surfaces of the clevis-pin as a combination of normal, tangential and shear stress components applied at points on internal surface with polar co-ordinates ϕ, z (Fig.1).

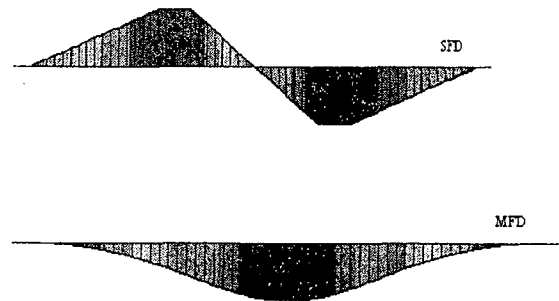


Fig. 2 : Shear force diagram and Bending moment diagram.

The output V_o of an ideal load cell should be a function of only the measured force F . The combination of stresses in the clevis-pin type load cell may be represented by:

$$\bar{\sigma} = \bar{\sigma}_b + \bar{\tau}_{\phi z} \quad (1)$$

where, σ_b is the longitudinal bending stress and can be expressed by:

$$\sigma_b = \frac{M\bar{y}}{I} \quad (2)$$

and $\tau_{\phi z}$ is the shear stress and can be expressed by:

$$\tau_{\phi z} = \frac{Q A \bar{y}}{I b} \quad (3)$$

where M = bending moment

Q = shear force

$A \bar{y}$ = moment of area of the section outward from the neutral axis further from that location of the shear stress

I = second moment of area

b = width of the cross section

Initially, consider only the effect of the stress component on the output of strain gauge aligned along the longitudinal axis of the load cell. The contribution of the shear stress ($\tau_{\phi z}$) will be the only applicable stress, as at the neutral axis the bending stress (σ_b) is zero.

From Hooke's law, the shear strain can be calculated by:

$$\gamma_{\phi z} = \frac{\tau_{\phi z}}{G} \quad (4)$$

where

$$G = \frac{E}{2(1 + \nu)}$$

In practice, the above equations do not accurately describe the behaviour of real hollow-bore load cells. The output of load cells are obtained from the combined output of strain gauges mounted in a pattern on the (internal) surface only.

3. Modelling of the clevis-pin

3.1 Modelling details

In this investigation, various kinds of geometric parameters for the clevis-pin have been created. These parameters were inner diameter (d), outside diameter (D), length (L), and the height (H_1 , H_2 and H_3) of the yoke as shown in Fig.3. The clevis-pin in this investigation will be considered to act as a beam. From many references, when the aspect ratio L/D of a beam in bending is such as to be considered to be a 'short beam', the numerical solutions and the results of practical experiment do not agree with engineers simple theory of bending. For the arrangement considered, aspect ratios, L/D of 1.5, 2.0, 3.0, 4.0, 5.0 and d/D ratios 1/3, 1/2, 2/3 and 4/5 initially were taken. The clevis-pin diametrical clearance within the loading components was constant at 0.1 mm. (50 micron on radius) and the length of pin (L) and the width of yoke were kept constant at 150 mm. and 40 mm. respectively.

To understand the bending effect of the yoke against 'its' own stiffness, various heights and the material properties have been taken. For the arrangement of height, the ratio of H_1/W was kept constant at 1.0. For the material property of the yoke, variations were made of the values of Young's Modulus of Elasticity as if the yoke were made of various materials.

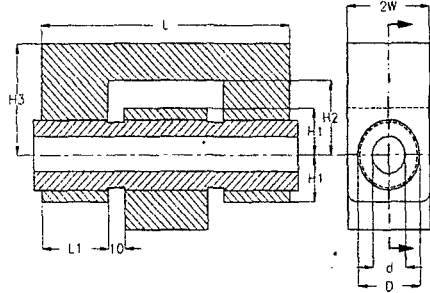


Fig. 3: Geometric parameters of clevis-pin.

3.2 Modelling Techniques

The models of the clevis-pin were generated and analysed using ANSYS version 5.4 finite element code. Because of symmetry, it was necessary to create only half-model. A three-dimensional analysis was performed using eight-node solid element (Solid 45) for both the clevis and the pin. Point-to-surface contact element (Contact 49) was applied with an elastic coulomb friction in the clevis-pin interface. To satisfy the symmetry condition, the nodes on yz plan (see Fig. 3) were constrained against x-displacement. The models were generated unconnectedly in order to prevent rigid-body motion. An incremental-iterative analysis was necessary to handle the geometrical nonlinearity caused by the clevis-pin contact condition. To solve and get reasonable solution, the contact stiffness (k) must be established and is acceptable to the program. A higher value of k will lead to ill-conditioning but the lower value may lead to convergence difficulties. The recommend formula for value of k is found from

$$k = f * E \quad (5)$$

Where f is a factor normally between 0.1 and 10

E is the Young modulus of contacting material (Use the smaller value for the different materials).

The applied load was divided into two steps, firstly to make a good contact by moving imposed displacement. This step was necessary to solve, otherwise the stiffness matrix $[K]$ of the connected bodies would become singular and unsolvable. This technique enabled the solution to converge rapidly by giving only one substep

and a small number of incremental times. The next step force F was applied to the model, this step was necessary divided into several substeps and the minimum and maximum of substeps permitted were set to 1 and 10 respectively in order to establish initial substep. Within each substep a maximum of 25 equilibrium iterations were allowed. To obtain a converged solution in a reasonable period of time, the force tolerance was set to 0.001. The penalty function was chosen to satisfy contactability and the contact condition was updated at each substep by using an iterative procedure to find the substep equilibrium state.

4. Results and Analysis

Some of the factors of influence are illustrated in Fig. 4. The geometric properties of length, diameter and bore-size, are of very direct influence. The factors analysed in this chapter were not completely exhaustive, rather, these factors were studied because of their obvious influence on the design of a hollow-bore clevis-pin type of load cell. The factors presented in this chapter are the gauge position (z and ϕ), the L/D and d/D ratios, the gauge element angle ($\pm\theta$), the stiffness of the yoke arms which involve both the geometry.

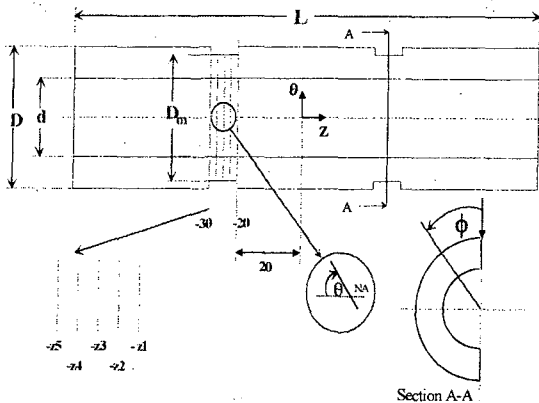
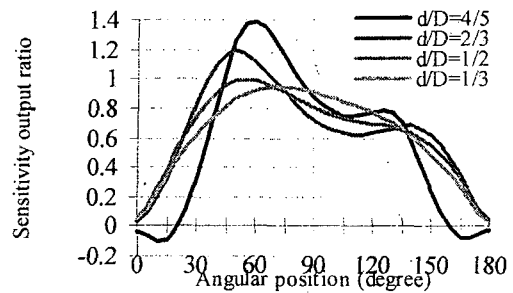


Fig. 4: The various variables defining the geometry of a hollow cylinder and the placement and orientation of the elements of the strain gauges.

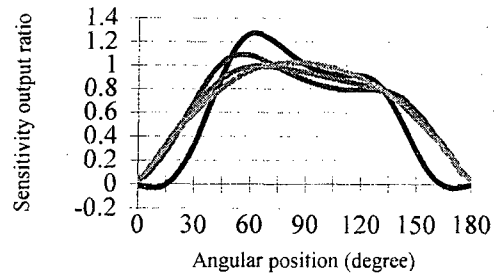
4.1 Effects of the gauge position (Z and ϕ)

Fig. 5a-d illustrates the sensitivity output, in ratio to the theoretical 'base' value, for various d/D ratios at the 'mid-way' station ratio $z/Z = 0.33$ when $L/D = 2, 3, 4$ and 5, and Fig. 6a-d presents the same results 'in reverse character' now for various kind of L/D ratios when $d/D = 4/5, 2/3, 1/2$ and $1/3$. As has already been discussed in the previous section, the results show that L/D of 4.0 and 5.0 (a longer design) and d/D of $1/2$ and $1/3$ (a thicker hollow cylinder) gave what some may judge to be 'better results' with more symmetry about the circumferential angle position of 90° and with a 'flatter-topped' character with circumferential angle. These features appear to offer more scope for tolerating any slight mis-position of the strain gauge elements in manufacture.

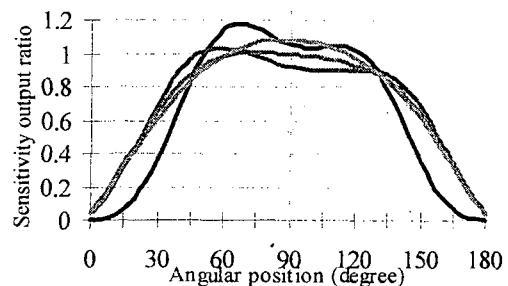
These benefits are less clear with ratios from L/D of 2.0 and 3.0 (a shorter design) and with d/D of $4/5$ and $2/3$ (a thinner hollow cylinder). At L/D of 2.0 for the angular angle of 90° , none of any d/D ratio give results close to the 'base value' but at L/D of 3.0, d/D of $1/2$ and $1/3$ a result closer to the base value is obtained. At L/D of 4.0 and 5.0, the 'best' d/D ratio to give the 'best results' at an angular position of 90° , were at d/D equal to $1/2$ and $1/3$. The results of these analyses, suggest that a hollow clevis-pin should have L/D ratio more than 3.0 and d/D ratio less than $1/2$ for the strain gauges being place at angular position of 90° . These conditions are not entirely met for some commercial designs.



a) $L/D = 2.0$



b) $L/D = 3.0$



c) $L/D = 4.0$

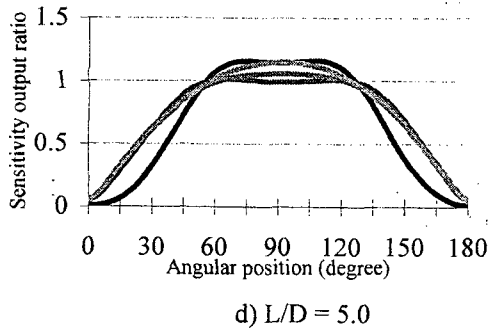


Fig. 5a-d: The sensitivity output ratio with various kind of d/D ratios.

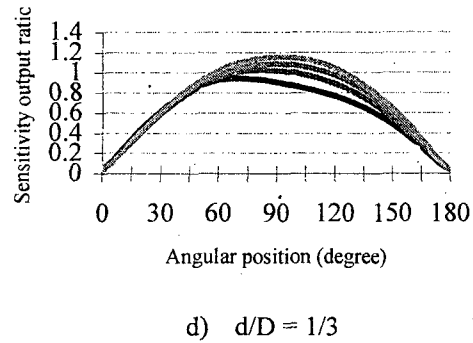
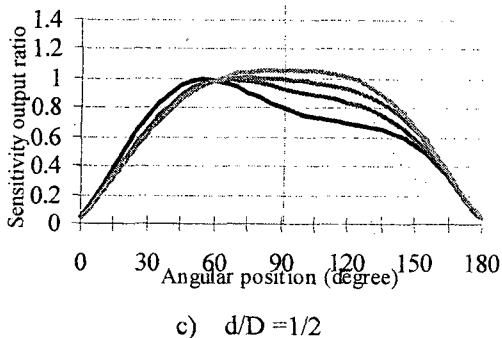
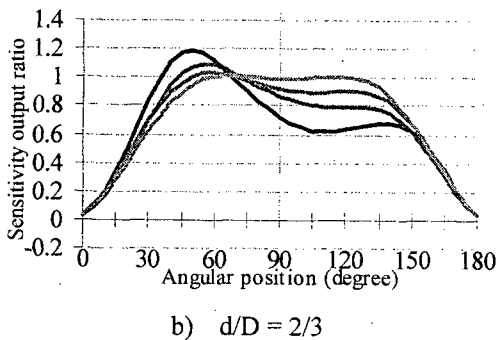
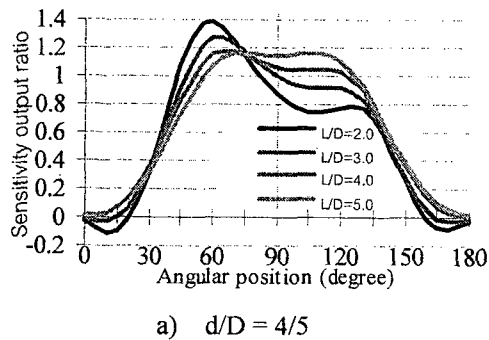


Fig. 6a-d: The sensitivity output ratio with various kind of L/D ratios.



4.2 Effects of yoke arm stiffness

The yoke arm is rotated by the in-plane rotational moments induced by the beam-like transverse deflection distortions of the clevis-pin. This rotation is resisted by the natural stiffness of the yoke arm but there may also be in-plane rotational distortions included in the arms of the yoke by any cranked path of the load in the yoke itself. So far, the analysis has been taken for an infinitely compliant yoke arm whose rotational action is free and unresisted. In practice, the in-plane rotational stiffness is real and significant. As a result, in-plane additional moments are imposed and the contact pressure pattern within the contact patch between clevis-pin and bore within the arms of the yoke becomes altered. The natural flow of the individual lines of unit force within the clevis-pin thereby become altered as the lines of force transverse through the clevis-pin to the central 'bushing' or loaded member. Fig. 7 illustrates the idealistic natural flow of the lines of force through a hollow pin.

There are number of factors that can cause a variation in the contact pressure patterns between the yoke and the clevis-pin. These factors are the aspect ratio of the yoke arm H_3/w , the width of the yoke arm and its loading position, and the yoke arm geometry and material in the structure some distance away from the clevis-pin.

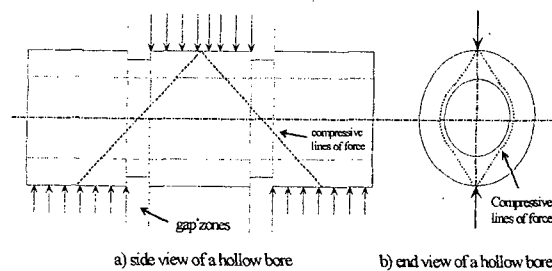


Fig. 7: Idealistic suggestion for the lines of force through a hollow pin.

4.3 Effects of the geometry for the yoke arm

In the analysis of this study, the effects of the yoke geometry have been divided into two main factors. These are the aspect ratio, H_3/w , and the ratio of the width of the yoke arm as well as the position of the loading in the

axial sense along the clevis-pin. Under an analysis of these circumstances, some models of a hollow clevis-pin are selected for study. Not only do good scientific principles require some extremes of the likely 'span' of characteristics to be presented, there is the very obvious requirement to cover what is practical. The variations of L/D found in commercial products are of range from 2.34 -3.68. There is some good reason to select for investigation L/D values of, say 2.5 and 4.0 for such extreme cases and perhaps L/D of 3.0 for the value of a ratio 'in between'. For the selection of thickness ratios for study, it is likely that a relatively thick wall ($d/D = 1/2$) is suitable. This thickness ratio is practical. There also appears to be some suggestion from the forgoing work of the earlier section that a 'best' gauge position might be at the middle of the 'gap zone' (Z -co-ordinate at $z/Z = 0.33$) and with an angular position of $\phi = 90^\circ$. This particular arrangement will be selected for further investigation.

4.4 Effects of various H_3/w ratios

Two geometric extremes of the yoke arms have been studied. Normally, the ratio H_3/w (Fig. 3) which is the ratio of the height to the half width of the yoke arm, is taken in practical application to be somewhere about 2. This is a relatively stiff arrangement with may be taken to have the yoke very much resisting the in-plane rotation of the end regions of the clevis-pin. On the other hand, the ratio H_3/w has been taken to be as large as 30. This case becomes near to the unrestrained case of simple support which has been already taken. Fig.8a and Fig.8b show the proportion taken for the two extremes, one has a 'massive' yoke to resist in-plane bending and another having a flexible yoke to approximate to that of providing a near 'simple support'. The study of the two extreme case of 'simple support' and 'built-in' (or nearly) will lead an understanding of effects of a spectrum (of 'fixity'). If the result show no significant difference between the two cases, it may seen that any aspect ratio of H_3/w falling in between can be applied.

Fig.9a and Fig.9b show the results of effects of various yoke arm aspect ratios (H_3/w). These results are plotted in terms of the sensitivity output comparing the results of the finite element method to those of the simple bending engineering theory on the surface of the bore of the clevis-pin. It can be seen that at the gauge position so far taken, (Z -direction at the middle of the gap zones and angle of $\phi = 90^\circ$ or perhaps a little greater) and for L/D ratio of 4.0, the results from very high ratios of H_3/w (the purple line) were almost at a ratio of 'unity' as were the results of the same proportion from section 6.2 (the pink line). The sensitivity hardly changed at all for wide changes the character of the yoke. However at other angular positions (ϕ), the sensitivity changes a little with variation in the stiffness of the yoke but the differences appear to be no greater than 10% at the worst. It may seen notable that at the 'normal' gauge position nearby ϕ of 90° , the results are simply that of the simple 'base' calculation and the effects of yoke stiffness appear to be of only very little account. For the other differences occurring in the strain signals appear very small in

following the form of that already discovered in the earlier. The results seem to suggest that the calibration of the strain gauged hollow-bore clevis-pin is unlikely to be changed very much by the restriction of in-plane distortion of the arms of the yoke.

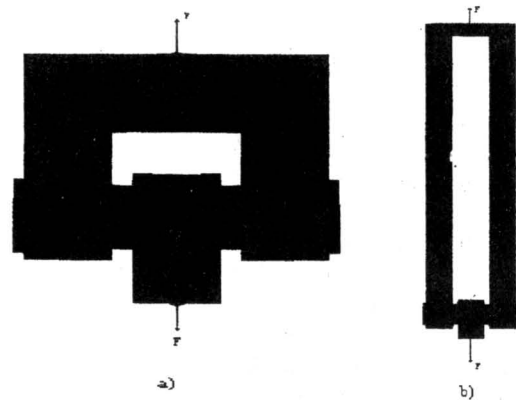
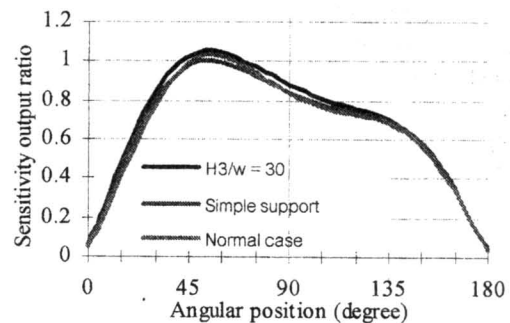
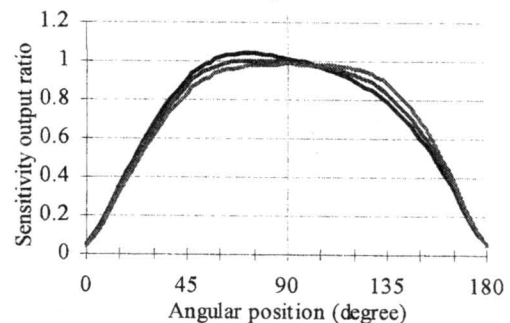


Fig.8: Distortion of the yoke arm when a) $H_3/w = 2.0$ (normal case), b) $H_3/w = 30.0$.



a) $L/D = 2.5, d/D = 1/2$



b) $L/D = 4.0, d/D = 1/2$

Fig.9a-b : The sensitivity output ratio variation with various 'aspect ratio' for yoke arm.

4.5 Other matters-stress and load capacity

It appears to have become the general rule that in the design of the elastic elements of strain gauged load cells, the maximum strain level experienced by the elastic element ought not to exceed a strain of the order about 1000 to 1500 microstrain. At these orders of strain level, experience seems to indicate that an acceptable level of mechanical linearity of behaviour and a low level of hysteresis can be obtained. The order of uncertainty

obtained in the complete load cell might thereby approach to 0.1 % of the intended full scale load (i.e. 1 microstrain in 1000 microstrain). It also appears that with suitable control of the metallurgy, this criterion of

It is a reasonably straight forward matter to design both the tension/compression and also the bending-beam type of strain gauged elastic element to each have this level of strain occurring directly underneath the position of the installed strain gauges and no where else. Indeed, on these two types of elastic element, there are advantages in deliberately arranging the load geometry to achieve a stress/strain 'concentrator' that has just this purpose.

In the hollow-bore clevis-pin, the strain gauges are to be placed in a plain part of the design and not necessarily directly where the maximum stress or strain are achieved. The 'gap zone' may be considered as a stress/strain concentrator, although it is not deliberately contrived for this reason. Even so, the maximum stress is likely to occur on the outer surface parts and not at the strain gauge positions in the hollow-bore.

It seems reasonable to consider that the complex bi-axial stress/strain field of the hollow-bore clevis-pin, no von-Mises equivalent stress ought to exceed that previously determined for the rather more simple forms of elastic element in the direct tension/compression or bending beam devices. The von-Mises equivalent stress on a free surface is given by:

$$\sigma_{\text{von-Mises}} = \sqrt{\sigma_1^2 + \sigma_2^2 + \sigma_1 \sigma_2} \quad (6)$$

σ_1, σ_2 being the principal stresses

Thus, for a simple tension or bending beam devices where the surface stress condition is uniaxial in nature ($\sigma_2 = 0$), the von-Mises limiting stress becomes that of the maximum principal stress viz.

$$\begin{aligned} &= 1500 \times 10^{-6} \times 207 \times 10^9 \times 10^{-6} \\ &= 311 \text{ MP} \end{aligned}$$

For some of the previously considered proportions of a hollow-bore clevis-pin, the von-Mises maximum stresses have been located and listed. The region of the 'gap zone' has in each case been proportioned with blend-radii at the 'step down' into the gap zone and the results have been tested for proper convergence with sufficiently fine meshing of the modulus in the appropriate region. The D_m/D ratio for each model was 0.9.

The three illustrations of Fig.10a-c show the pictorial representations from the finite element computations for the three model proportions. All had d/D of 1/2 with $L = 150 \text{ mm}$. The load was 5000 N in a 'simple support' type of support. The locations of the maximum von-Mises stress in the gap zone are indicated along with the region underneath the pattern of strain gauges. Table 1 gives the relevant values.

precision can be equally obtained with both the special hardenable steel and aluminium alloy commonly used in elastic elements.

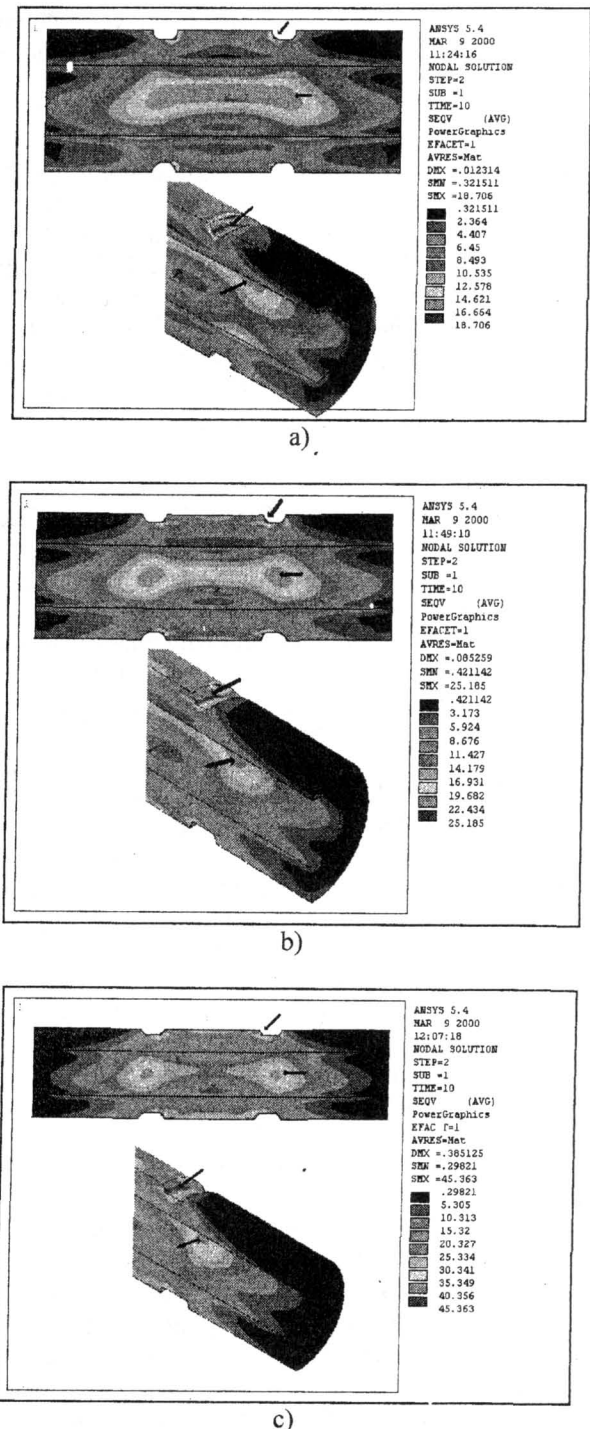


Fig.10: Illustration the von-Mises stress equivalent plot of a model having a) $L/D = 2.5$, $d/D = 1/2$, b) $L/D = 3.0$, $d/D = 1/2$, c) $L/D = 4.0$, $d/D = 1/2$ subjected to the applied load of 5,000 N (simple support case).

| Von-Mises stress etc. | L/D ratio with L = 150 mm. | | |
|---|----------------------------|-------|-------|
| | 2.5 | 3.0 | 4.0 |
| at $\phi = 90^\circ$ | 15.8 | 21.7 | 38.9 |
| Maximum elsewhere | 18.7 | 25.2 | 45.4 |
| Maximum allowed | 311 | 311 | 311 |
| Ratio at $\phi = 90^\circ$ to max. elsewhere | 0.85* | 0.86* | 0.86* |
| $\frac{\sigma_{\text{vonMises, allowed}}}{\sigma_{\text{vonMises, max}}}$ | 16.6 | 12.3 | 6.9 |

Table 1: von-Mises stress equivalent stress

The results seem to show that for the proportions shown, the stress level at the gauge position is likely to be about $0.85 \times$ that of the maximum stress elsewhere and which would set the maximum condition limiting the satisfactory performance of a hollow-bore clevis-pin.

The results also show that the somewhat arbitrary choice of 5000 N as a load for investigation of the author, as a criterion of structural stressing, might have been increased considerably. Supposing that a proportion of $L/D = 4.0$ had been chosen, a maximum load of perhaps $6.9 \times 5 \text{ kN} = 35 \text{ kN}$. Might have been contemplated, all other matters being of lesser significance.

5. Conclusions

The work and study on which this thesis is based has been concerned with the hollow-bore clevis-pin as a strain gauge load cell. The results have shown:

- The proportions are likely to be of length to diameter ratio varying from about 2.5: 1 to about 3.5:1 or perhaps 4.0:1.
- The best results are likely to be obtained with bore to outside diameter (in the gap zone) ratio giving thick-wall proportions and, typically, of from 1/2 to 1/3.
- With the suggested proportions, the best placement for the companion positions of the strain gauge coupons is within the hollow-bore on opposite sides of a diameter perpendicular to the line-of-action of the applied load.
- There is a need to ensure adequate clearances in fit between the clevis-pin and the mounting bores. These clearances are best described as of somewhat general proportions in engineering terms.

6. Suggestion for future work

The work of the author has involved the investigation and testing of over 200 separate finite element models. Nonetheless, it has not proved possible to investigate all the possible features and particularly the possible combination of features. Perhaps the most notable feature suggested for future work concerns the sensitivity and performance of hollow-bore clevis-pin load cells to the diametrical clearances in the fit to the mating parts. There are two aspects to this viz:

- (i) where the existing design of machinery or structure dictates the size of the clevis-pin that it

is possible to fit, and the stressing of the clevis-pin is considerable,

- (ii) where either the existing design of machinery or structure produces a relatively light loading on the size of the replacement clevis-pin in direct fit or the existing design of machinery or structure allows a free choice for the size (diameter) of the clevis-pin to be fitted.

7. References.

- [1] Abdullah, F. and Erdem, U., 'Mathematical Modelling and Design of a Shear Force Load Cell Transducer', VDI-Berichte Nr.312, 1978, page 149-155.
- [2] Bahra, C. S. and Evans, J. W., 'Strain Gauge Loadcell Design and Use', Transducer Tempcom Conference Papers, Trident International Exhibitions, Tavistock, Devon, UK, 1983, page 1-22.
- [3] Barbato, G., Desogus, S., Zompi A. and Levi, R., 'Load-cell-design Developments by Numerical and Experimental Methods', Experimental Mechanics, September 1981, page 341-348.
- [4] Bray, A., 'The Role of Stress Analysis in the Design of Force-standard Transducers', Experimental Mechanics, January 1981, page 1-20.
- [5] Bray, A. and Levi, R., Theory and Practice of Force Measurement, Academic Press Limited, London, UK, 1990.
- [6] Dally, J. W. and Riley, W. F., Experimental Stress Analysis, McGraw-Hill, Inc., 1978.
- [7] Doebelin, E.O., Measurement Systems: Application and Design, McGraw-Hill, Inc., USA, 1966.
- [8] Erdem, U., 'Force and Weight Measurement', Journal of Physics. Part E: Science Instrumentation, Vol. 15, 1982, page 857-872.
- [9] Hearn, E.J., Mechanics of Materials Vol.1&2, Pergamon Press Ltd., Oxford, England, 1985.
- [10] Hill, D.A., Nowell, D. and Sackfield, A., Mechanics of Elastic Contacts, Oxford: Butterworth-Heinemann, 1993.
- [11] Kutsay, U.S. Patent No. 3,695,096 'Strain Detecting Load Cell', USA, 3 October 1972.
- [12] Loos, U.S. Patent No. 4,454,769 'Radial Force Measurement Cell', UAS, 19 June 1984.
- [13] Measurement Group, Inc., Experimental Stress Analysis 'NOTEBOOK', issue 6, May 1987.
- [14] Pascoe, S. K., Contact Stress Analysis Using Finite Element Methods, Ph.D. Thesis, Department of Mechanical Engineering, University of Liverpool, 1990.
- [15] Piyasin, S., The Design of the Hollow-bore Clevis-Pin type of Load Cell, Ph.D. Thesis, Department of Mechanical Engineering, University of Sheffield, March 2000.
- [16] Roark, R. J. and Young, W. C., Formulas for Stress and Strain, 5th Edition, McGraw-Hill, Kogakusha, LTD., 1975.

- [17] Robinson, G.M., Genetic Algorithm Optimisation of Load cell Geometry by Finite Element Analysis, PhD Thesis, City University, London, 1995.
- [18] Swanson Analysis System, Inc., ANSYS User's Manual for Revision 5.0 Vol.1, DN-R300:50-1,1992.
- [19] Swanson Analysis System, Inc., ANSYS User's Manual for Revision 5.0 Vol.4, DN-R300:50-4,1992.
- [20] Swanson Analysis System, Inc., Structural Nonlinearities-User's Guide for Revision 5.1 Vol. 2, DN-S201:51-2, 1995.
- [21] Taylor, D.A.W., Strain Gauge Transducers, Short course notes, Department of Mechanical Engineering, University of Sheffield.
- [22] Technical Staff of Measurements Group, Inc., Strain Gage Based Transducers-Their design and construction, Measurements Group, Inc., Raleigh, North Carolina 27611, USA, 1988.
- [23] Transducer Techniques, Load Cells Force/Torque Sensors' Catalogue, USA, 1999